Hindawi Publishing Corporation
Journal of Spectroscopy
Volume 2015, Article ID 329730, 7 pages
http://dx.doi.org/10.1155/2015/329730

Research Article

Raman Spectroscopy and Electrochemical Investigations of Pt Electrocatalyst Supported on Carbon Prepared through Plasma Pyrolysis of Natural Gas

Tereza Cristina Santos Evangelista,[1] Giordano Toscano Paganoto,[1] Marco Cesar Cunegundes Guimarães,[2] and Josimar Ribeiro[1]

[1]*Departamento de Química, Centro de Ciências Exatas, UFES, Avenida Fernando Ferrari, 514 Goiabeiras, 29075-910 Vitória, ES, Brazil*
[2]*Departamento de Morfologia, Centro de Ciências da Saúde, UFES, Campus de Maruípe, 29049-999 Vitória, ES, Brazil*

Correspondence should be addressed to Josimar Ribeiro; josimar.ribeiro@ufes.br

Received 17 March 2015; Revised 8 July 2015; Accepted 15 July 2015

Academic Editor: Christophe Dujardin

Physicochemical and electrochemical characterisations of Pt-based electrocatalysts supported on carbon (Vulcan carbon, C1, and carbon produced by plasma pyrolysis of natural gas, C2) toward ethanol electrooxidation were investigated. The $Pt_{20}/C1_{80}$ and $Pt_{20}/C2_{80}$ electrocatalysts were prepared by thermal decomposition of polymeric precursors at 350°C. The electrochemical and physicochemical characterisations of the electrocatalysts were performed by means of X-ray diffraction (XRD), transmission electron microscope (TEM), Raman scattering, cyclic voltammetry, and chronoamperometry tests. The XRD results show that the Pt-based electrocatalysts present platinum metallic which is face-centered cubic structure. The results indicate that the $Pt_{20}/C1_{80}$ electrocatalyst has a smaller particle size (10.1–6.9 nm) compared with the $Pt_{20}/C2_{80}$ electrocatalyst; however, the $Pt_{20}/C2_{80}$ particle sizes are similar (12.8–10.4 nm) and almost independent of the reflection planes, which suggests that the Pt crystallites grow with a radial shape. Raman results reveal that both Vulcan carbon and plasma carbon are graphite-like materials consisting mostly of sp^2 carbon. Cyclic voltammetry and chronoamperometry data obtained in this study indicate that the deposition of Pt on plasma carbon increases its electrocatalytic activity toward ethanol oxidation reaction.

1. Introduction

Global warming and methods to avoid it have been the topics of much recent debate. Fear of exhausting fossil fuel-based energy sources, the price and supply crises for this type of fuel, and clean and renewable energy policies have motivated alternative energy sources. Such concerns support implementing of the fuel cells, which were discovered by Sir William Grove in 1839 and are a form of efficient electricity generation with low environmental impact [1, 2].

Ethanol has been used as a fuel and is much less toxic, compared with methanol; and the technology involved in the manufacture of the ethanol fuel cell is similar to that of direct methanol cells [3]. In Brazil, ethanol production is especially efficient; the industry maintains such production through a well-structured methodology due to the use of ethanol as vehicle fuel over several decades [4].

A support material commonly used in electrocatalyst for fuel cells is the Vulcan carbon. This type of carbon is widely employed in electrocatalyst preparation because it has a surface area that facilitates maximum nanoparticle dispersion and adequate electrocatalyst pore distribution. Moreover, the pore size and functional groups on the carbon surface are also critical for its use as an electrocatalyst support [5]. Recently, different kinds of carbon nanomaterials such as hollow graphitic nanoparticles [6], carbon nanotubes [7],

and graphitic carbon nanofibers [6] were investigated and different fabrication methods have been adopted. These carbon materials can exhibit superior performance compared to the conventional carbon supports for EOR (ethanol oxidation reaction) anode catalysts. Carbon materials usually have a high surface area to disperse metal grains, and their high conductivity transfers electrons generated from electrochemical reactions taking place on the anode [8].

Tang et al. [9] reviewed new carbon materials such as ordered porous carbon and carbon nanofibers, which have been used in direct alcohol fuel cells. According to them, these materials generally presented better performance due to their special structure, better crystallinity, good stability, and faster mass transfer compared to the commercial carbon nanotubes materials [10]. Moreover, it has been shown that carbon can also be produced by plasma pyrolysis of natural gas [11]. This method is a promising way of producing high-purity black carbon without generation of environmentally harmful products [11]. Upon plasma pyrolysis, methane decomposes to produce hydrogen and a solid carbon rich residue commonly designed as "black plasma" [12, 13].

The Pt-based electrocatalysts are the most used on Polymer Membrane Fuel Cells (PMFC) for oxidation of hydrogen [14, 15] as well as low molecular weight organic molecules such as methanol [16, 17], ethanol [18, 19], ethylene glycol [20, 21], and dimethyl ether [22, 23]. These fuels have been widely investigated not only in fundamental research but also in several commercial corporations [24]. However, the high cost and the scarcity of Pt form a great border in PMFC's development. A fundamentally interesting feature of these Pt-based electrocatalysts is their size and morphology dependent electrocatalytic activity [25]. It is well known that pure Pt can be readily poisoned by CO-like intermediate species produced in the alcohol oxidation reaction [26, 27]. Therefore, it is very important to investigate new low loading of Pt materials that not only can improve the CO-tolerance of Pt, but also enhance its catalytic activity for alcohol oxidation.

Thus, the aim of this paper was to prepare Pt-based electrocatalysts on Vulcan carbon, C1, and carbon produced by plasma pyrolysis of natural gas, C2; then, the electrocatalyst activity toward ethanol electrooxidation was compared.

2. Experimental Section

2.1. Synthesis of Pt/C Electrocatalysts by Thermal Decomposition of Polymeric Precursors (DPP). Thermal decomposition of polymeric precursors (DPP) was used to prepare Pt/C electrocatalysts with a nominal composition, $Pt_{20}/C1_{80}$ and $Pt_{20}/C2_{80}$ (where C1 is the Vulcan carbon, purchased from Carbot Corporation and C2 is a carbon produced by plasma pyrolysis of natural gas, which was provided by Prof. Dr. Alfredo Gonçalves Cunha).

The Pt polymeric precursor resin, Pt-resin, was synthesised by mixing citric acid (CA) in ethylene glycol (EG) in the proportion 1 : 4 at 60–65°C. After the citric acid was fully dissolved in ethylene glycol, 50 mL of a solution of metal precursor salt (H_2PtCl_6, Aldrich) dissolved in isopropanol (~0.02 mol/L) was slowly added to the CA/EG mixture. After the solution was fully added, the H_2PtCl_6/CA/EG mixture temperature was raised to 80–85°C for esterification. The H_2PtCl_6/CA/EG mixture was kept under stirring for 0.5–1 h, which generated the desired Pt-resin. The Pt-resin produced using this method was stable and can be stored at room temperature; the resin metal concentration was determined using inductively coupled plasma optical emission spectrometry (ICP-OES) with the Pt-resin = 3.8×10^{-4} mol Pt/g resin.

The Pt/C electrocatalysts dispersed on carbon (C1, Vulcan carbon, or C2, plasma carbon) with the mass ratio 20 wt.% platinum and 80 wt.% carbon were prepared by adding the respective Pt-resin precursors at levels corresponding to the desired compositions ($Pt_{20}/C1_{80}$ and $Pt_{20}/C2_{80}$). Two millilitres of ethanol was added to the mixture to aid dispersion in an ultrasonic bath for 30 minutes. Both the $Pt_{20}/C1_{80}$ and $Pt_{20}/C2_{80}$ electrocatalysts were annealed at 350°C in an air atmosphere for 3 hours using an oven.

2.2. Physicochemical Characterisations of Pt/C Electrocatalysts. Physicochemical characterisation included X-ray diffraction (XRD) using a Bruker D8 advance with CuKα radiation (λ = 1.5406 Å) and 2θ scanning from 20° to 90° (step = 0.03° and step time = 3 s). The crystallite sizes (d) were determined using the Scherrer equation (1), as follows [28]:

$$d = \frac{0.9 \times \lambda}{B \times \cos\theta}, \quad (1)$$

where B is the reflection width at half-maximum intensity and θ is the angle at the maximum intensity.

The two different carbon and Pt/C electrocatalysts were analysed through Raman spectroscopy using a Witec Confocal Raman Microscope System Alpha 300R. The Raman analyses were performed over the material using a neon laser incidence at 533 nm and the wavenumbers range 0–4000 cm^{-1}.

The morphology and dispersion of Pt/C electrocatalyst particles were investigated using a JEOL/JEM-1400 transmission electron microscope (TEM) operated at 200 kV.

2.3. Electrochemical Characterisations of Pt/C Electrocatalysts. Electrochemical characterisations were performed using 0.5 mol dm^{-3} H_2SO_4 (Aldrich) as the supporting electrolyte in ultra-pure water (18 MΩ cm at 20°C). The graphite electrode (4 cm^2 geometric area) and reference $Ag/AgCl_{KClsat}$ electrode were used as the counter and reference electrodes, respectively.

The working electrode was prepared through deposition on a carbon substrate previously polished using alumina (0.3 μm) and 30 μL of a Pt/C electrocatalyst solution, which was prepared by dispersing 1 mg of electrocatalyst in ethanol (190 μL) and Nafion (10 μL). The materials electrocatalytic activities were evaluated through cyclic voltammetry (CV), which was recorded in the −100 mV to 1000 mV versus $Ag/AgCl_{KClsat}$ potential range with and without 1.0 mol dm^{-3} ethanol (Aldrich) and chronoamperometry at 400 mV versus $Ag/AgCl_{KClsat}$ for 2 hours. The electrochemical experiments were performed at room temperature in a one-compartment electrochemical cell (body, 50 mL) using an AUTOLAB 302N model potentiostat/galvanostat.

Table 1: XRD results for the two different Pt/C electrocatalysts prepared using the DPP process. C1, Vulcan carbon, and C2, plasma carbon.

Electrocatalyst	Phase	a (Å)	V (Å^3)	d/nm				
				111	200	220	311	222
$Pt_{20}/C1_{80}$	Pt	3.921 ± 0.001	60.3 ± 0.1	10.1	7.7	7.6	7.4	6.9
$Pt_{20}/C2_{80}$	Pt	3.923 ± 0.001	60.4 ± 0.1	12.8	10.8	10.4	10.4	11.5

a_{Pt} = 3.920 Å [29].

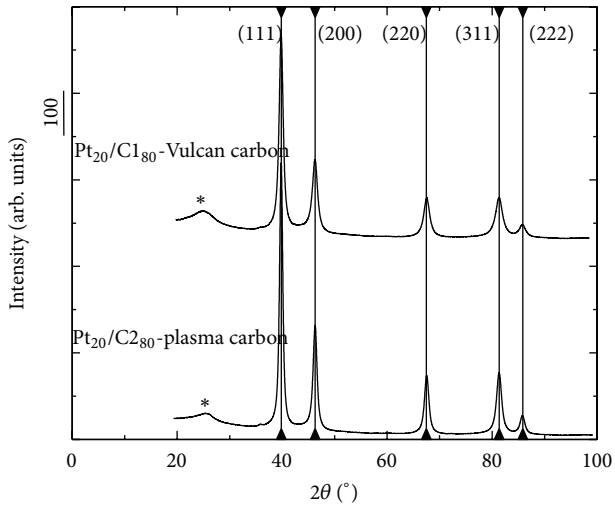

Figure 1: XRD patterns of Pt/C electrocatalysts prepared through the DPP process and dispersed on Vulcan carbon or plasma carbon (20 wt.% Pt loading).

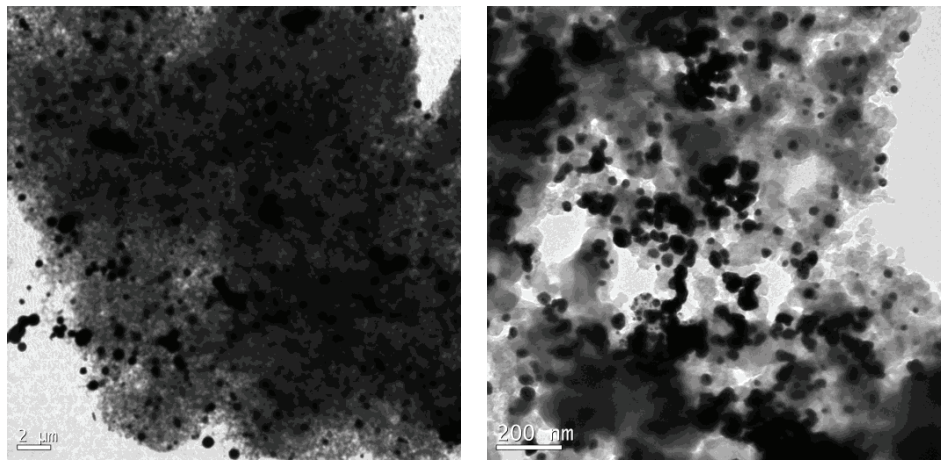

(a) (b)

Figure 2: TEM images of Pt/C electrocatalysts dispersed on Vulcan carbon (a) and plasma carbon (b).

3. Results and Discussion

Figure 1 shows the XRD patterns for the $Pt_{20}/C1_{80}$ and $Pt_{20}/C2_{80}$ electrocatalysts, which were prepared by thermally decomposing the polymeric precursors. The carbon support (peak at $2\theta = 25^\circ$) was detected. The XRD patterns show the primary peaks for a face-centred cubic (FCC) crystalline Pt (PDF: 01-087-0646 [29]) with (111), (200), (220), and (311) diffraction planes. The crystallite sizes were measured using Scherrer's equation [28], and the results are shown in Table 1. The results indicate that the $Pt_{20}/C1_{80}$ electrocatalyst has a smaller particle size (10.1–6.9 nm) compared with the $Pt_{20}/C2_{80}$ electrocatalyst. However, the $Pt_{20}/C2_{80}$ particle sizes are similar (12.8–10.4 nm) and almost independent of the diffraction planes, which suggests that the Pt crystallites grow with a radial shape.

The TEM images for both $Pt_{20}/C1_{80}$ and $Pt_{20}/C2_{80}$ electrocatalysts are shown in Figure 2. One can see that the

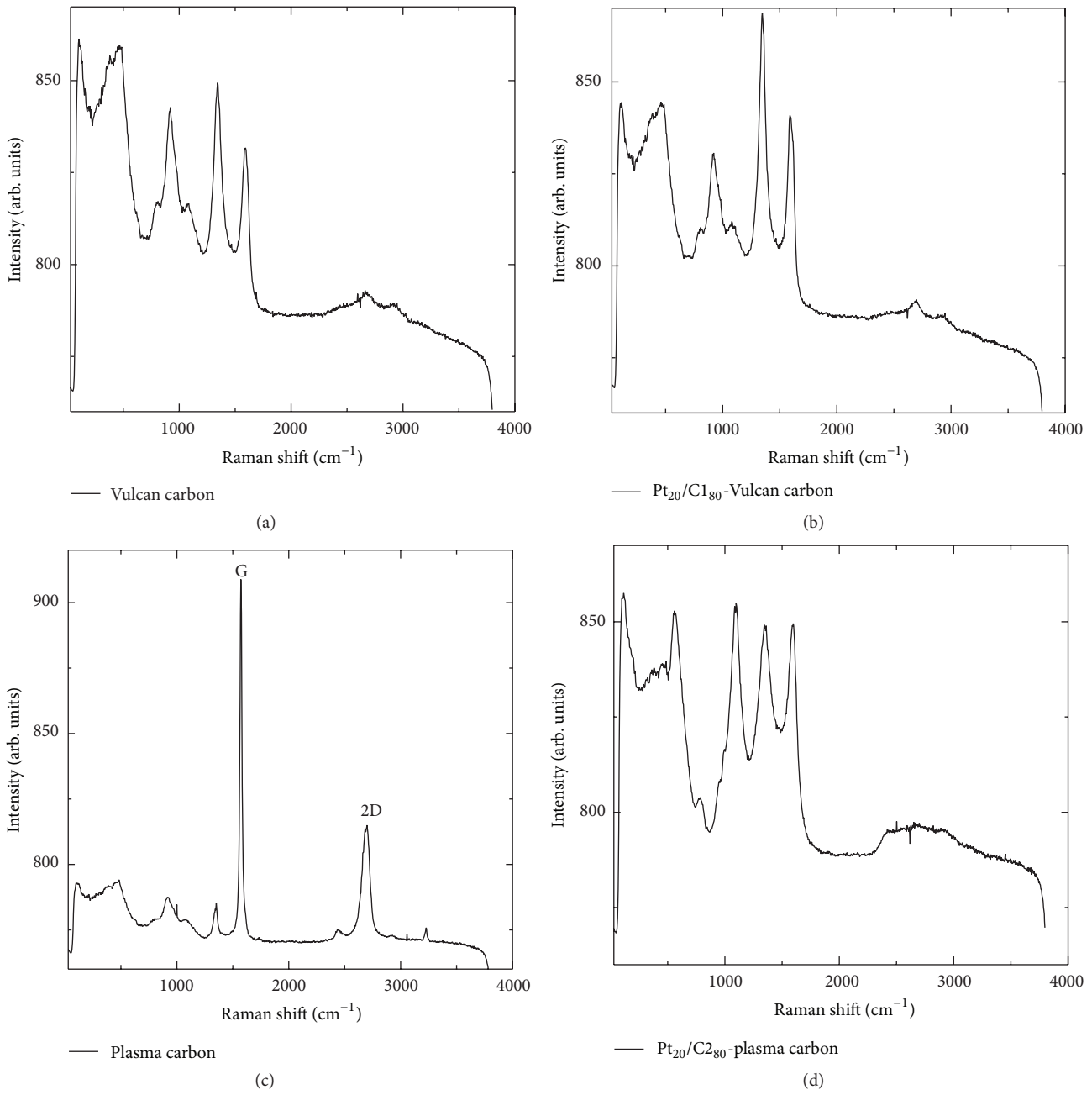

Figure 3: Raman spectra of the carbon and Pt/C electrocatalysts prepared through the DPP process.

particles are not well dispersed on C1 support. The higher particle density and particle size in $Pt_{20}/C2_{80}$ electrocatalyst strongly suggest that nucleation is promoted in this sample. Because this effect occurs in the Vulcan carbon support, one can infer that surface defects in this material act as enhanced nucleation sites for Pt DPP process. However, the electrocatalyst $Pt_{20}/C2_{80}$ is well dispersed and its particle size (average *ca.* 6.1 nm) agrees with XRD data. It is obvious from these results that the particle size of Pt increases when the Vulcan carbon is used as material support compared with the plasma carbon, which leads to some undesirable agglomeration of the particles.

Figure 3 shows the Raman spectra of carbon materials and Pt/C electrocatalyst prepared by DPP process. The well-known peaks of carbon graphite [30–32], which are the primary features, were observed for all materials investigated with varying levels of intensity and width in the 1350 and 1590 cm^{-1} regions, respectively. Moreover, in the carbon plasma sample (Figure 3(c)), the other strong band near 2680 cm^{-1}, corresponding to a 2D mode, is a relatively sharp peak that can be associated with a graphene layer [33]. However, in the $Pt_{20}/C2_{80}$ sample, this strong band disappears; it might be due to Pt nanoparticles presence or to a thermal treatment during DPP process. The intensity of

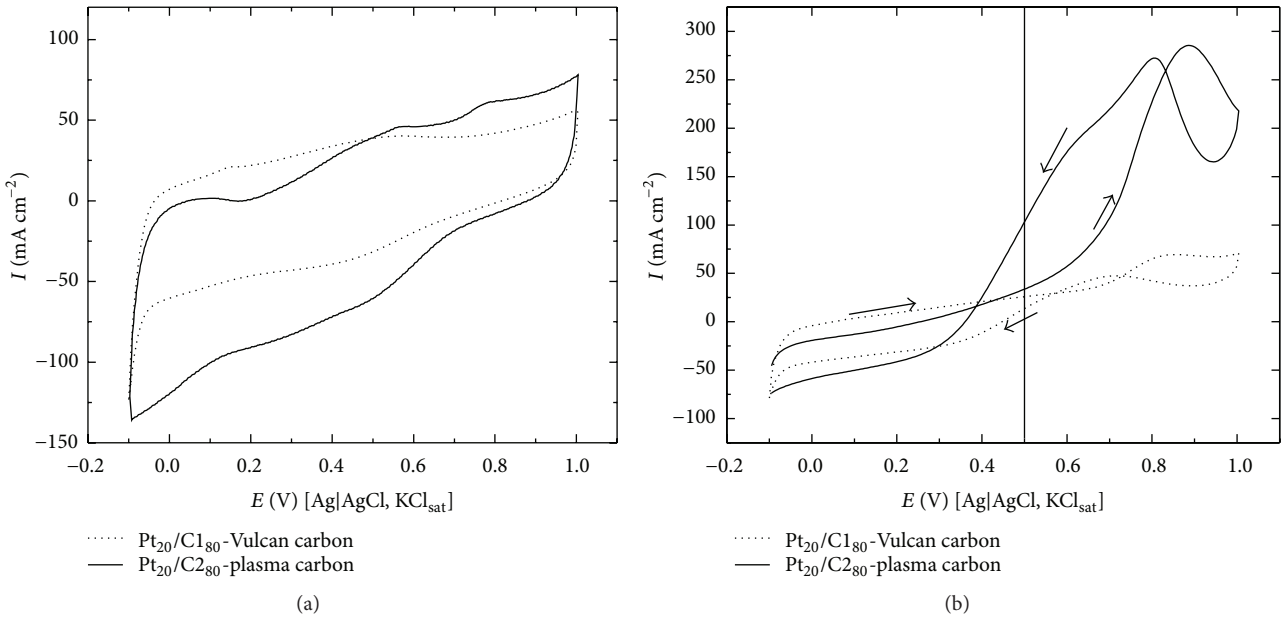

Figure 4: (a) Cyclic voltammograms of Pt/C electrocatalysts in 0.5 mol dm^{-3} H_2SO_4 at 20 mV s^{-1} and (b) cyclic voltammograms of the Pt/C electrocatalysts in 0.5 mol dm^{-3} H_2SO_4 + 1.0 mol dm^{-3} ethanol at 20 mV s^{-1}. (Dotted line) $Pt_{20}/C1_{80}$-Vulcan carbon and (solid line) $Pt_{20}/C2_{80}$-plasma carbon.

G peak (~1580 cm^{-1}) and ratio $I(2D)/I(G)$ in Figures 3(a) and 3(c), respectively, reveals that both Vulcan carbon and plasma carbon are graphite-like materials consisting mostly of sp^2 carbon [34].

Figure 4(a) shows the cyclic voltammograms (CV) for the two Pt/C electrocatalysts deposited on a carbon substrate in 0.5 mol dm^{-3} H_2SO_4. The CV curves are distorted compared with that of pure Pt (data not shown here). Moreover, the hydrogen oxidation region (from −0.10 to 0.20 V versus $Ag/Ag/Cl_{KClsat}$) for both $Pt_{20}/C1_{80}$ and $Pt_{20}/C2_{80}$ electrocatalysts does not show the typical adsorption/desorption peaks, conversely to the case of Pt/C with 40% metal loading published by us before [35]. The obtained CV profile, suggesting a partially blocked Pt surface, may be due to the incomplete decomposition of carbonaceous species from DPP process. The $Pt_{20}/C2_{80}$ has a larger double layer region compared with $Pt_{20}/C1_{80}$ electrocatalysts, which may be associated with surface higher area in the plasma carbon than in the Vulcan carbon, because it is well known that carbon is responsible for large capacitive responses.

Cyclic voltammograms for oxidation of the ethanol adsorbed on the Pt/C electrocatalysts are compared in Figure 4(b). The cyclic voltammetry curves for ethanol show three peaks: one during the positive-going scan (Vulcan carbon E = 0.84 V versus $Ag/Ag/Cl_{KClsat}$; I = 68.9 mA cm^{-2}, and plasma carbon E = 0.88 V versus $Ag/Ag/Cl_{KClsat}$; I = 284.6 mA cm^{-2}) which is attributed to the ethanol oxidation and two oxidation peaks observed during the negative-going scan which is associated with the removal/or oxidation of intermediates species (e.g., CO, C_xH_y, and $C_xH_yO_z$) not completely oxidized in the positive-going scan [21]. The ethanol begins to oxidise at ~0.4 V versus $Ag/Ag/Cl_{KClsat}$, and the electrocatalyst fuel oxidation efficiency can be analysed; ethanol oxidation is more efficient where the oxidation potential is lower and the current density is higher (demonstrated using the CV) [35]. For example, if one fixes the potential at 0.5 V versus $Ag/Ag/Cl_{KClsat}$ one gets the following current density values: Vulcan carbon: $I_{forward}$ = 26.4 mA cm^{-2} and $I_{backward}$ = 14.4 mA cm^{-2}; plasma carbon: $I_{forward}$ = 33.2 mA cm^{-2} and $I_{backward}$ = 103.4 mA cm^{-2}. Thus, one can infer that $Pt_{20}/C2_{80}$ displays better performance than $Pt_{20}/C1_{80}$ electrocatalysts and this behavior indicates a possible structure effect in the Pt electrocatalytic activity. The structure effect in the Pt electrocatalytic activity in the EOR has been demonstrated by other studies on well-ordered [36, 37] as well as nanostructured surfaces [38, 39].

Figure 5 represents the chronoamperometry (CA) curves recorded at a constant potential of 400 mV versus $Ag/AgCl_{KClsat}$ for two hours. CA allowed evaluation of the electrocatalysts activity of the electrocatalysts. This is a typical exponential decay observed in any step-potential technique; however, one can observe that, during the first minutes, there is a sharp decrease in the current density normalized by Pt loading for the $Pt_{20}/C1_{80}$ electrocatalyst, followed by a slow decrease in the I-values at 2500 s, which become very lower after this period time. This behavior could be explained by strong adsorption of the intermediates CO, CH_x, and $C_xH_yO_z$ type residues on the Pt active sites, which is causing the poisoning of the surface. It is well known in the literature that CH_x and CO species could poison the platinum sites during the alcohol electrooxidation reaction [26, 27, 40]. However, for the $Pt_{20}/C2_{80}$ electrocatalyst, the behavior is very different; one can see that current density normalized by Pt loading decreases slowly for longer time

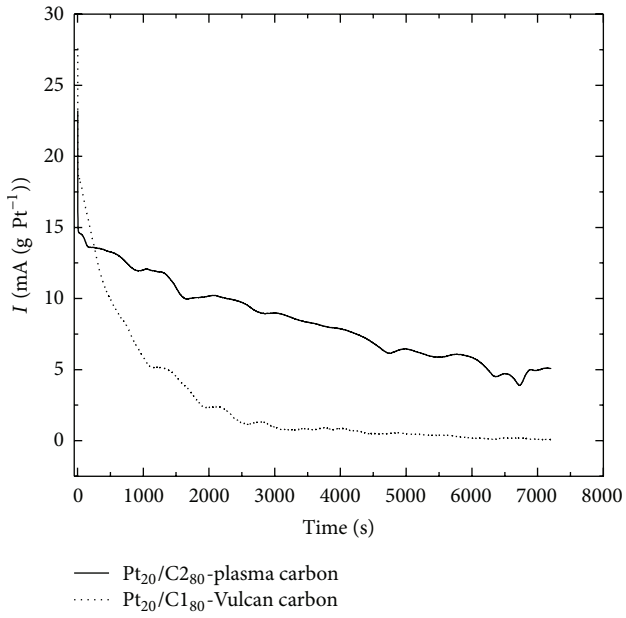

Figure 5: Current versus time curves for the electrooxidation 1.0 mol dm^{-3} ethanol in 0.5 mol dm^{-3} H_2SO_4 at 400 mV versus $Ag/AgCl_{KClsat}$ for 2 hours on Pt/C electrocatalysts. (Dotted line) Pt_{20}/Cl_{80}-Vulcan carbon and (solid line) $Pt_{20}/C2_{80}$-plasma carbon. Current values normalized by the Pt loading.

periods. In this case, the main cause of slow current-time decay is not due to poisoning of the platinum sites but is due to the surface instability of nanoparticles, because of the surface recrystallisation, surface metal segregation, particle agglomeration, and so forth, decreasing slowly the number of active sites of the electrocatalysts [35]. The $Pt_{20}/C2_{80}$ electrocatalyst furnished the best result in this test, because to the end of the experiment the I-values obtained for the $Pt_{20}/C2_{80}$ (5 mA/gPt) are higher than for the Pt_{20}/Cl_{80} electrocatalyst.

4. Conclusions

This paper has shown that Pt-based electrocatalysts can be prepared using carbon produced using a plasma torch from natural gas vehicles. XRD results indicate that the Pt_{20}/Cl_{80} electrocatalyst has a smaller particle size (10.1–6.9 nm) compared with the $Pt_{20}/C2_{80}$ electrocatalyst (12.8–10.4 nm). Moreover XRD data obtained for $Pt_{20}/C2_{80}$ suggests that the Pt crystallites grow with a radial shape. Raman results showed that all the materials are composed of randomly oriented structural units varying from 50 to 80 Å in size. The voltammetry for the $Pt_{20}/C2_{80}$ electrocatalyst showed better charge density and current, compared with the Pt_{20}/Cl_{80} electrocatalyst. Finally, CA experiment has demonstrated that $Pt_{20}/C2_{80}$ electrocatalyst furnished the best result, thus demonstrating its enhanced oxidative capacity for ethanol.

Conflict of Interests

The authors declare that there is no conflict of interests regarding the publication of this paper.

Acknowledgments

J. Ribeiro especially acknowledges FAPES and CNPq for financial support. The authors also acknowledge CAPES, FINEP, LMC, and PETROBRAS.

References

[1] U.S. Department of Energy. Office of Fossil Energy. National Energy Technology Laboratory, *Fuel Cell Handbook*, EG&G Technical Services, 7th edition, 2004.

[2] T. Iwasita, "Fuel cells: Spectroscopic studies in the electrocatalysis of alcohol oxidation," *Journal of the Brazilian Chemical Society*, vol. 13, no. 4, pp. 401–409, 2002.

[3] D. Wang, J. Liu, Z. Wu et al., "Electrooxidation of methanol, ethanol and 1-propanol on pd electrode in alkaline medium," *International Journal of Electrochemical Science*, vol. 4, no. 12, pp. 1672–1678, 2009.

[4] L. C. Basso, H. V. de Amorim, A. J. de Oliveira, and M. L. Lopes, "Yeast selection for fuel ethanol production in Brazil," *FEMS Yeast Research*, vol. 8, no. 7, pp. 1155–1163, 2008.

[5] S. K. Meher and G. R. Rao, "Morphology-controlled promoting activity of nanostructured MnO_2 for methanol and ethanol electrooxidation on Pt/C," *Journal of Physical Chemistry C*, vol. 117, no. 10, pp. 4888–4900, 2013.

[6] X. S. Zhao, W. Z. Li, L. H. Jiang et al., "Multi-wall carbon nanotube supported Pt–Sn nanoparticles as an anode catalyst for the direct ethanol fuel cell," *Carbon*, vol. 42, no. 15, pp. 3263–3265, 2004.

[7] E. J. Yoo, T. Okata, T. Akita, M. Kohyama, J. Nakamura, and I. Honma, "Enhanced electrocatalytic activity of Pt subnanoclusters on graphene nanosheet surface," *Nano Letters*, vol. 9, no. 6, pp. 2255–2259, 2009.

[8] H. Wu, D. Wexler, and H. Liu, "Pt-Ni/C catalysts using different carbon supports for the cathode of the proton exchange membrane fuel cell (PEMFC)," *Materials Chemistry and Physics*, vol. 136, no. 2-3, pp. 845–849, 2012.

[9] S. Tang, G. Sun, J. Qi et al., "New carbon materials as catalyst supports in direct alcohol fuel cells," *Chinese Journal of Catalysis*, vol. 31, no. 1, pp. 12–17, 2010.

[10] Y. Wang, C. He, A. Brouzgou et al., "A facile soft-template synthesis of ordered mesoporous carbon/tungsten carbide composites with high surface area for methanol electrooxidation," *Journal of Power Sources*, vol. 200, pp. 8–13, 2012.

[11] J. C. C. Freitas, D. F. Cipriano, C. G. Zucolotto, A. G. Cunha, and F. Emmerich, "Solid-state NMR study of carbon blacks obtained by plasma pyrolysis of natural gas," in *Proceedings of the Annual World Conference on Carbon*, Krakow, Poland, 2012.

[12] L. Fulcheri and Y. Schwob, "From methane to hydrogen, carbon black and water," *International Journal of Hydrogen Energy*, vol. 20, no. 3, pp. 197–202, 1995.

[13] J. R. Fincke, R. P. Anderson, T. A. Hyde, and B. A. Detering, "Plasma pyrolysis of methane to hydrogen and carbon black," *Industrial and Engineering Chemistry Research*, vol. 41, no. 6, pp. 1425–1435, 2002.

[14] P. E. Dodds, I. Staffell, A. D. Hawkes et al., "Hydrogen and fuel cell technologies for heating: a review," *International Journal of Hydrogen Energy*, vol. 40, no. 5, pp. 2065–2083, 2015.

[15] E. Antolini and E. R. Gonzalez, "The electro-oxidation of carbon monoxide, hydrogen/carbon monoxide and methanol in acid medium on Pt-Sn catalysts for low-temperature fuel

cells: a comparative review of the effect of Pt-Sn structural characteristics," *Electrochimica Acta*, vol. 56, no. 1, pp. 1–14, 2010.

[16] F. L. S. Purgato, L. A. Montoro, J. Ribeiro, K. B. Kokoh, and P. Olivi, "The effect of heat treatment on the preparation of Pt-RuO_2/C electrocatalysts," *Electrocatalysis*, vol. 1, no. 2-3, pp. 122–128, 2010.

[17] L. Li and Y. Xing, "Pt-Ru nanoparticles supported on carbon nanotubes as methanol fuel cell catalysts," *Journal of Physical Chemistry C*, vol. 111, no. 6, pp. 2803–2808, 2007.

[18] S. S. Gupta and J. Datta, "A comparative study on ethanol oxidation behavior at Pt and PtRh electrodeposits," *Journal of Electroanalytical Chemistry*, vol. 594, no. 1, pp. 65–72, 2006.

[19] A. Brouzgou, S. Q. Song, and P. Tsiakaras, "Low and non-platinum electrocatalysts for PEMFCs: current status, challenges and prospects," *Applied Catalysis B: Environmental*, vol. 127, pp. 371–388, 2012.

[20] A. Serov and C. Kwak, "Recent achievements in direct ethylene glycol fuel cells (DEGFC)," *Applied Catalysis B: Environmental*, vol. 97, no. 1-2, pp. 1–12, 2010.

[21] F. E. Teran, D. M. Santos, J. Ribeiro, and K. B. Kokoh, "Activity of PtSnRh/C nanoparticles for the electrooxidation of C1 and C2 alcohols," *Thin Solid Films*, vol. 520, no. 18, pp. 5846–5850, 2012.

[22] A. Serov and C. Kwak, "Progress in development of direct dimethyl ether fuel cells," *Applied Catalysis B: Environmental*, vol. 91, no. 1-2, pp. 1–10, 2009.

[23] I. Mizutani, Y. Liu, S. Mitsushima, K.-I. Ota, and N. Kamiya, "Anode reaction mechanism and crossover in direct dimethyl ether fuel cell," *Journal of Power Sources*, vol. 156, no. 2, pp. 183–189, 2006.

[24] X. Zhang, H. Zhu, Z. Guo, Y. Wei, and F. Wang, "Design and preparation of CNT@SnO_2 core-shell composites with thin shell and its application for ethanol oxidation," *International Journal of Hydrogen Energy*, vol. 35, no. 17, pp. 8841–8847, 2010.

[25] W.-P. Zhou, M. Li, C. Koenigsmann, C. Ma, S. S. Wong, and R. R. Adzic, "Morphology-dependent activity of Pt nanocatalysts for ethanol oxidation in acidic media: nanowires versus nanoparticles," *Electrochimica Acta*, vol. 56, no. 27, pp. 9824–9830, 2011.

[26] A. R. Bonesi, M. S. Moreno, W. E. Triaca, and A. M. C. Luna, "Modified catalytic materials for ethanol oxidation," *International Journal of Hydrogen Energy*, vol. 35, no. 11, pp. 5999–6004, 2010.

[27] F. Kadirgan, S. Beyhan, and T. Atilan, "Preparation and characterization of nano-sized Pt-Pd/C catalysts and comparison of their electro-activity toward methanol and ethanol oxidation," *International Journal of Hydrogen Energy*, vol. 34, no. 10, pp. 4312–4320, 2009.

[28] D. Cullity and S. R. Stock, *Elements of X-Ray Diffraction*, Prentice Hall, Upper Saddle River, NJ, USA, 3rd edition, 2001.

[29] *Powder Diffraction File: 01-087-0646*, vol. PDF-2, Joint Committee on Powder Diffraction Standards, International Center for Diffraction Data, Newtown Square, Pa, USA, 2011.

[30] R. Escribano, J. J. Sloan, N. Siddique, N. Sze, and T. Dudev, "Raman spectroscopy of carbon-containing particles," *Vibrational Spectroscopy*, vol. 26, no. 2, pp. 179–186, 2001.

[31] F. Tunistra and J. L. Koenig, "Raman spectrum of graphite," *The Journal of Chemical Physics*, vol. 53, no. 3, pp. 1126–1130, 1970.

[32] R. S. Das and Y. K. Agrawal, "Raman spectroscopy: recent advancements, techniques and applications," *Vibrational Spectroscopy*, vol. 57, no. 2, pp. 163–176, 2011.

[33] A. C. Ferrari and J. Robertson, "Interpretation of Raman spectra of disordered and amorphous carbon," *Physical Review B*, vol. 61, no. 20, pp. 14095–14107, 2000.

[34] A. C. Ferrari, J. C. Meyer, V. Scardaci et al., "Raman spectrum of graphene and graphene layers," *Physical Review Letters*, vol. 97, no. 18, Article ID 187401, 2006.

[35] J. Ribeiro, D. M. dos Anjos, K. B. Kokoh et al., "Carbon-supported ternary PtSnIr catalysts for direct ethanol fuel cell," *Electrochimica Acta*, vol. 52, no. 24, pp. 6997–7006, 2007.

[36] D. J. Tarnowski and C. Korzeniewski, "Effects of surface step density on the electrochemical oxidation of ethanol to acetic acid," *Journal of Physical Chemistry B*, vol. 101, no. 2, pp. 253–258, 1997.

[37] A. A. Abd-El-Latif, E. Mostafa, S. Huxter, G. Attard, and H. Baltruschat, "Electrooxidation of ethanol at polycrystalline and platinum stepped single crystals: a study by differential electrochemical mass spectrometry," *Electrochimica Acta*, vol. 55, no. 27, pp. 7951–7960, 2010.

[38] Z.-Y. Zhou, Z.-Z. Huang, D.-J. Chen, Q. Wang, N. Tian, and S.-G. Sun, "High-index faceted platinum nanocrystals supported on carbon black as highly efficient catalysts for ethanol electrooxidation," *Angewandte Chemie—International Edition*, vol. 49, no. 2, pp. 411–414, 2010.

[39] S. Singh and J. Datta, "Kinetic investigations and product analysis for optimizing platinum loading in direct ethanol fuel cell (DEFC) electrodes," *Ionics*, vol. 17, no. 9, pp. 785–798, 2011.

[40] M. L. Calegaro, H. B. Suffredini, S. A. S. Machado, and L. A. Avaca, "Preparation, characterization and utilization of a new electrocatalyst for ethanol oxidation obtained by the sol-gel method," *Journal of Power Sources*, vol. 156, no. 2, pp. 300–305, 2006.